CERAMICS — Silikáty 35, s. 97—112 (1991)

Original papers

THE MAIN TECHNOLOGICAL CHARACTERISTICS OF GLASS TANK MELTING ZONES FROM THE STANDPOINT OF THE COURSE OF THE MELTING PROCESS

PART V. THE EFFECT OF BUBBLING ON THE COURSE OF FLOW

LUBOMÍR NĚMEC

Institute of the Chemistry of Glass and Ceramic Materials, Czechoslovak Academy of Sciences, Lípová 5, 120 00 Prague 2

Received 10. 4. 1990

The present study deals semiquantitatively with two cases of flow arrangement by means of bubbling, and with the effect of the arrangement on specific power consumption and the throughput of the melting zone. The arrangements consisted of several transverse rows of bubbling nozzles in the melting zone, and of one longitudinal row along the melting zone axis respectively. The results indicate a very favourable effect of such arrangement on the melting characteristics as well as on the melting conditions: the power consumption was significantly reduced and the throughput substantially increased, so that the melting temperature could have been decreased. However, an investigation of the two cases likewise revealed some problems and restrictions which can only be resolved on the basis of a precise knowledge of the flow arrangement. This is why the way leads to mathematical models of melting zones which will allow the problems to be resolved in a general manner.

INTRODUCTION

The results obtained so far in parts [1—4] permit the conditions of melting in an actual glass tank to be estimated from the standpoints of favourable power consumption as well as throughput. The numerical values for model equipment, particularly with respect to throughput at high temperatures, are very advantageous, but one cannot of course expect the results to be so positive with an actual glass tank. This is in particular due to certain simplifications there, introduced, such as the assumption of piston flow, that of isothermal melting cf. [4], and that of melting without the so-called melting reserve. Practical attainability of the favourable conditions is another problem to be resolved. Whereas the precisioning of suitable sand grain sizes or refining agent concentration is no difficult task, the use of a suitable mean melting temperature, a suitable dead zone size or bubbling represent demanding technological requirements that cannot always be met at the same time. For example, it is difficult to attain a high mean temperature in a large tank; on the other hand, bubbling can mostly not be carried out in a small tank. Often we do not succeed in affecting favourably the value of m.

THEORETICAL

Glass melting in a 'long' tank with transverse rows of nozzles

As an example of the possible ways of resolving the problem of melt flow in the melting zone, we will deal, at least approximately, with the case when the melt is bubbled by several rows of nozzles in succession at a lower or medium temperature, and in the next section heated to a high refining temperature and rapidly refined. This arrangement leads to a substantially better utilization of the melting zone [5] and the mixing effect will also favourably affect the sand dissolution process [6]. The case of several bubbling barriers was dealt with theoretically in [7]. The advantages of this application can be summarized as follows:

1. It is possible to estimate the character of flow and thus also the relationship between $\bar{\tau}$ and τ_0.
2. Bubbling affects favourably the rate of sand dissolution, as proved by laboratory experiments.
3. Bubbling affects favourably both power consumption and tank throughput, as proved by preliminary calculations on the model device (cf. Fig. 13 in Part [3]).
4. The fact that bubbling is nowadays currently used in glassmaking practice and the arrangement suggested can be readily realized on the basis of existing operational experience.

Study [7] gives the following equation for the mean concentration of sand particles passing from the l-th row of bubbling nozzles:

$$X_{m,\,l+1} = \sum_{i=1}^{m_0} A_{il} N'_{i+1} (1 - P')^{i-l} P'^{l+1}. \qquad (1)$$

On substituting for $X_{m,\,l+1}$ the standard allowable concentration of undissolved sand particles beyond the l-th row, $X_{m,\,l+1} = X_N$, then the value of P' in equation (1) gives the highest possible rate of flow through the nozzle row, allowing the standard requirement to be met. For piston flow it holds that

$$\bar{\tau} = (\tau_i / P')\, l. \qquad (2)$$

The value of $\bar{\tau}$ can then be used in the calculation of Q and P.

In the concrete case, let us consider a melting zone 10 m in length and 4 m in width, with a glass melt layer 1 m in thickness. The batch is charged in the front part (2 m) in length, and the surface in this part is completely covered with a batch layer. The remaining part of the melting zone is below a ceiling which is 0.1 m above the surface level. Although such a tank would have some disadvantages compared to standard industrial types, their elimination would make the calculation too complex and anyway would not affect the results to any considerable degree.

In the case of the use of bubbling, altogether ten transverse rows of nozzles are placed in the melting zone behind the batch layer (from the 2nd meter). It is assumed that the time of sand dissolution in the tank corresponds to the times of dissolution obtained while bubbling the glass melt under laboratory conditions. It is further assumed that the rate of flow in the model does not depend on the distance from the side walls, that the melt is of model type and that isothermal conditions prevail in the melting zone. Following the dissolving of sand, the refining is assumed to proceed at the advantageous refining temperatures established by

laboratory experiments (jump-wise temperature increase is considered for the sake of simplicity).

The material of the walls, their thickness and specific heat losses due to dissipation through the batch layer are the same as in the case of the model device [1]. The refining takes place in the elongated melting zone which has the same sectional area. For the course of refining it is assumed that at the refining temperature, the bubble should ascend through the entire height of the glass melt, i. e. 1 m. Melting without reserves is again assumed. The arrangement will be compared

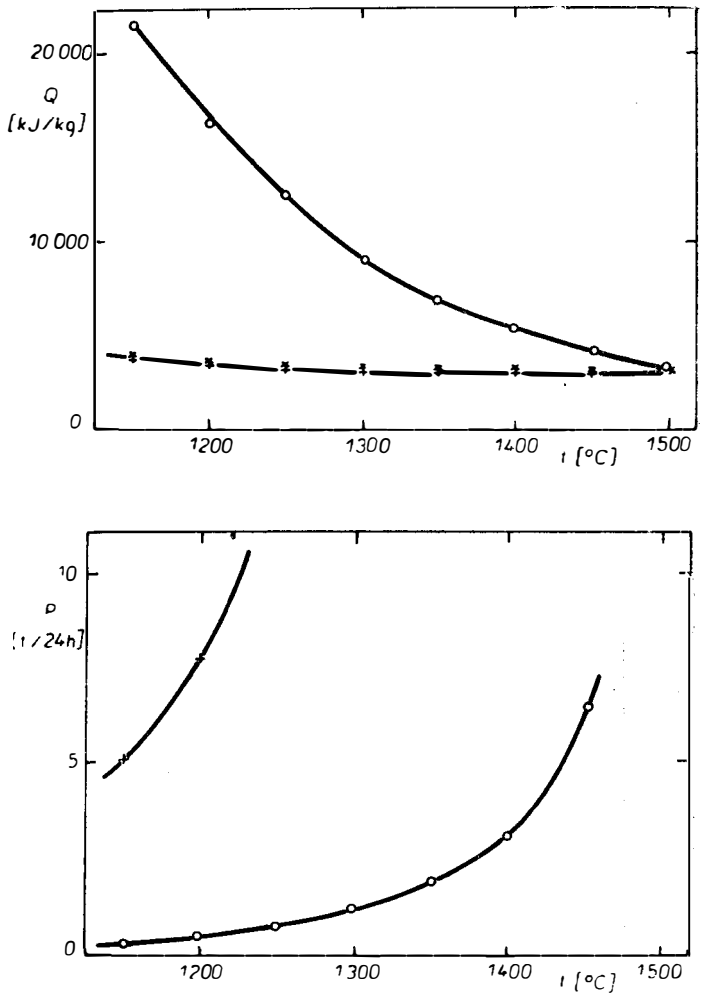

Fig. 1. Specific energy consumption and throughput in terms of temperature for a 'long tank', mode glass melt (74 % SiO_2, 16 % Na_2O, 10 % CaO), 0.7 % Na_2O as Na_2SO_4, r_{max} = 0.20 mm.

○ — *without bubbling,* $m_1 = 0.9$; $m_2 = 0$
× — *with bubbling,* $m_1 = 0$; $m_2 = 0.9$
\+ — *with bubbling,* $m_1 = 0$; $m_2 = 0$

with melting under isothermal conditions, in a furnace of the same shape but without bubbling, and with refining at the same temperature as in the former case.

For the calculation, $X_N = 1$ grain of sand per kilogram of glass melt is taken as the standard value, the τ_i is chosen constant for all the rows of nozzles, either $\tau_i = 240$ s or 220 s (the values are approximate and calculated from the literary data [8]). The values of A_i were taken over from [7]. The dependence of the number of undissolved sand grains on the number of circulations (the values of $N'_i(\tau_i)$) were obtained from the plots of experimental dependence of the number of undissolved sand grains on time for the individual cases. The tables of $N'_i(\tau_i)$ for the instances studied are not given here for reasons of brevity. The value of P' was

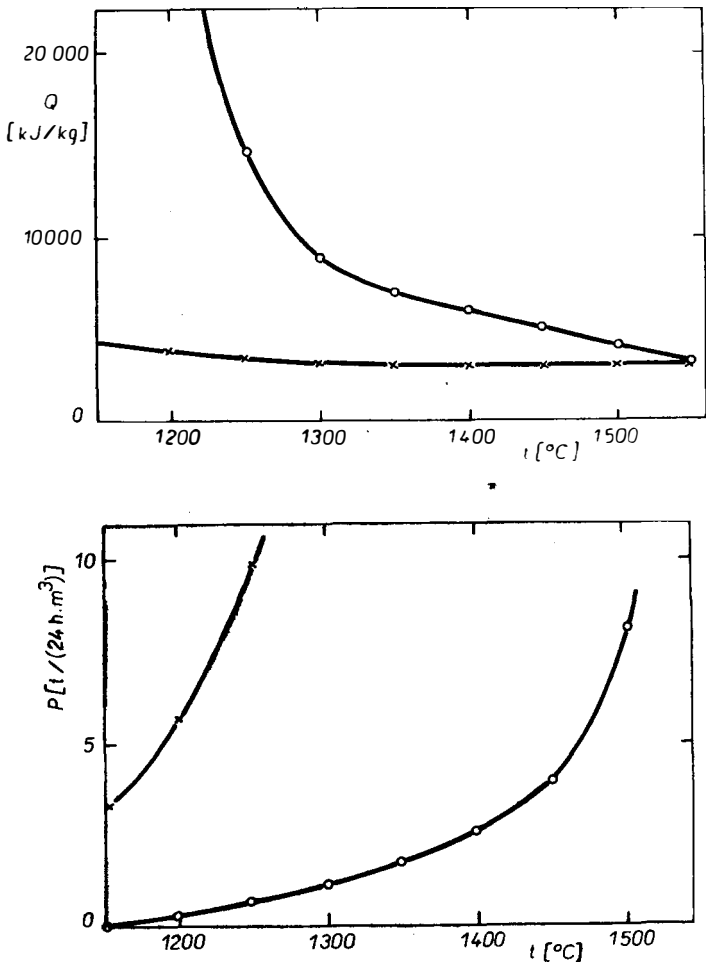

Fig. 2. Specific energy consumption and throughput in terms of temperature for a 'long tank', model glass melt, 2 % Na_2O as NaCl, $r_{0max} = 0.20$ mm.
○ — *without bubbling,* $m_1 = 0.9$; $m_2 = 0$
\+ — *with bubbling,* $m_1 = 0$; $m_2 = 0$

calculated from equation (1) by means of a computer. The respective development diagram is given in ref. [9] on page 53.

The following cases were studied:

1. The temperature dependence of Q and P in melting a model glass refined with 0.7 % Na_2O in the form of Na_2SO_4 (an advantageous concentration of the refining agent), $r_{0\,max.} = 0.20$ mm.

2. The temperature dependence of Q and P in melting a model glass refined with 2 % Na_2O in the form of NaCl (an advantageous concentration of the refining agent), $r_{0\,max.} = 0.20$ mm.

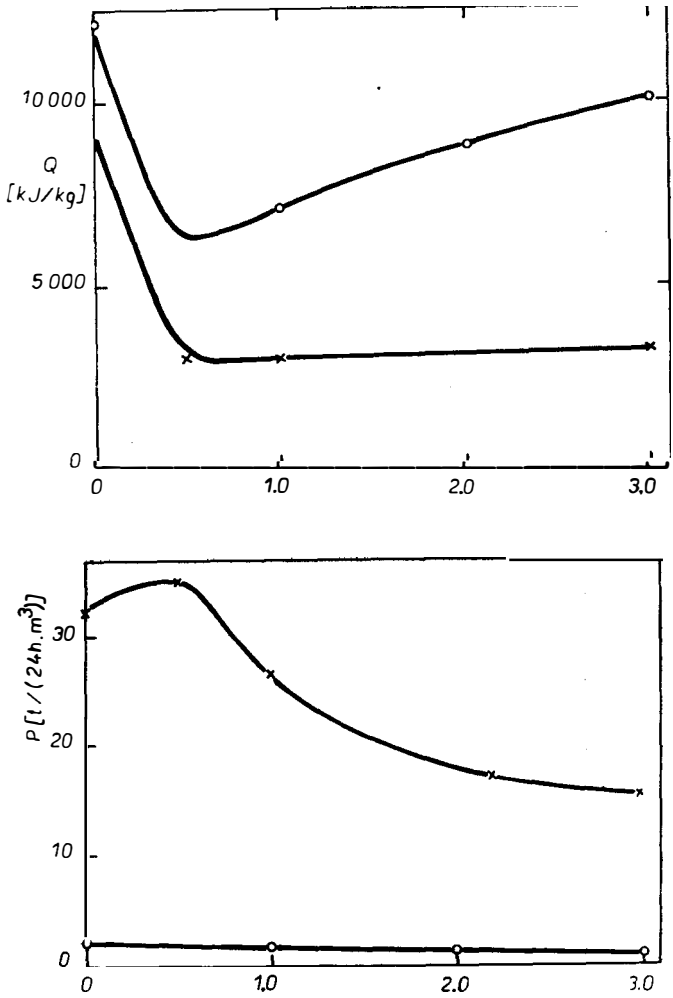

Fig. 3. Specific energy consumption and throughput in terms of NaCl *concentration (as* NaCl*) for a 'long tank', model glass melt, 1300 °C,* $r_{0max} = 0.20$ mm.

○ — *without bubbling,* $m_1 = 0.9$; $m_2 = 0$
× — *with bubbling,* $m_1 = 0$; $m_2 = 0$

3. The dependence of Q and P on the concentration of NaCl for melting the model glass refined with NaCl, $r_{0\,max.} = 0.20$ mm, $t = 1\,300$ °C.

Ad 1. The values of P' and $\bar{\tau}$ for this case are listed in Table I. Calculation according to equation (13) in [9] yields the time of refining, $\tau_R = \tau_2 = 740$ s, the respective losses according to equation (1), part [3], are $Q_{12} = 30.9$ kJ/kg ($m = 0$). Table II lists the calculated total values of specific power consumption and throughput for the cases being compared, according to equations (2) and (3), cf. Part [3]. The results are plotted in Fig. 1 and demonstrate the advantage of bubbling with respect to specific energy consumption as well as throughput.

Table I

The values of P' and $\bar{\tau}$ from equations (1) and (2)

t [°C]	1 150	1 200	1 250	1 300	1 350	1 400	1 450	1 500
P'	0.055	0.085	0.14	0.24	1.0	1.0	1.0	1.0
$\bar{\tau}$ [s]	39 636	25 647	15 571	9 083	5 070*	5 070*	5 070*	5 070*

*... $P'_{max} = 0.43$ [7]

Table II

The values of Q and P for the model glass melt refined with 0.7 % Na_2O in the form of Na_2SO_4, $r_{0\,max} = 0.20$ mm, the case without bubbling ($m_1 = 0.9$) and that with bubbling ($m_1 = 0$). (m_1 is the dead zone in the melting section)

		Without bubbling ($m_1 = 0.9$)		With bubbling ($m_1 = 0$)	
t [°C]	ΔQ_M [kJ/kg]	Q [kJ/kg]	P [t/(24 h m³)]	Q [kJ/kg]	P [t/(24 h m³)]
1 150	475	21 612	0.29	3 743	5.02
1 200	400	16 414	0.44	3 448	7.75
1 250	330	12 463	0.69	3 196	12.71
1 300	250	8 955	1.20	3 007	21.71
1 350	180	7 239	1.85	2 885	38.77
1 400	105	5 830	3.02	2 905	38.68
1 450	30	4 408	6.52	2 926	38.60
1 500	0	3 317	32.50	2 990	38.51

Table III

The values of P' and τ from equations (1) and (2)

t [°C]	1 200	1 250	1 300	1 350	1 400	1 450	1 500	1 530
P'	0.069	0.12	0.21	0.36	1.0	1.0	1.0	1.0
τ [s]	34 782	20 000	11 428	6666	5 581	5 581*	5 581*	5 581*

*... $P'_{max} = 0.43$ [7]

Table IV

The values of Q and P for the model glass melt refined with 2 % Na_2O in the form of NaCl, $r_{0\,max}$ = 0.20 mm, the case without bubbling (m_1 = 0.9) and with bubbling (m_1 = 0)

		Without bubbling (m_1 = 0.9)		With bubbling (m_1 = 0)	
t [°C]	ΔQ_M [kJ/kg]	Q [kJ/kg]	P [t/(24 h m³)]	Q [kJ/kg]	P [t/(24 h m³)]
1 150	585	108 870	0.05	4 358	3.31
1 200	490	35 050	0.18	3 795	5.70
1 250	420	14 490	0.53	3 415	9.89
1 300	340	8 887	1.17	3 172	17.27
1 350	270	7 204	1.78	3 024	29.55
1 400	195	6 152	2.56	2 997	35.21
1 450	120	5 151	3.99	3 025	35.14
1 500	45	4 002	8.15	3 043	35.06
1 530	0	3 021	40.6	3 063	34.98

Table V

The values of P' and $\bar{\tau}$ from equations (1) and (2) and the values of Q and P for the model glas melt refined with NaCl, $r_{0\,max}$ = 0.20 mm, 1 300 °C, the case without bubbling (m_1 = 0.9) and with bubbling (m_1 = 0)

		Without bubbling			With bubbling	
% Na_2O as NaCl	P'	$\bar{\tau}$ [s]	Q [kJ/kg]	P [t/(24 h m³)]	Q [kJ/kg]	P [t/(24 h m³)]
0	0.39	6 153	12 203	2.43	9 472	32.08
0.5	0.43*	5 581	6 429	2.03	3 085	35.37
1.0	0.32	7 500	7 159	1.64	3 053	26.32
2.0	0.21	11 428	8 887	1.17	3 172	17.27
3.0	0.19	12 631	10 102	0.98	3 228	15.63

* ... P'_{max}

Ad 2. The values of P and $\bar{\tau}$ for this case are given in Table III. Calculation according to equation (13) in ref. [9] yields the time of refining $\tau_R = \bar{\tau}_2$ = 272 s, the respective losses with the use of equation (1) in Part [3] being Q = 15 kJ/kg (m = 0). Table IV presents, according to equations (2) and (3), Part [3], the calculated overall values of specific energy consumption and throughput for the two cases being compared. The results, as plotted in Fig. 2, likewise prove the advantages of bubbling with respect to Q and P. One can also observe a great similarity with the case in Fig. 1.

Ad 3. Similarly, the concentration dependence of Q and P for the two cases was also calculated. The results are listed in Table V. The values of Q and P plotted in Fig. 3 demonstrate the advantages of bubbling at 1300 °C over a wide concentration range of the refining agent. The only unfavourable case is that not using any refining agent because the considerable increase in the time of refining is responsible for a considerable rise in the Q value and the length of the refining zone.

'Long tank' with a central lengthwise row of nozzles

The facts given in the previous chapter and in [4] point out the great significance of a favourable flow for both energy consumption and throughput of the melting furnace. This is obviously due to reducing the very unfavourable ratio $\bar{\tau}/\tau_{\text{pass}}$, which amounts to 8—10 with current types of tanks but should be equal to unity in the ideal case. A reduction of the ratio would be significant particularly with classical melting tanks operated at not too high mean temperatures (the reduction of losses being significant from the standpoint of energy consumption). The case dealt with in the previous chapter and in ref. [7] was aimed above all at reducing the $\bar{\tau}/\tau_{\text{pass}}$ ratio by introducing transverse flow by means of bubbling nozzles. For the case that $\tau_{\text{pass}} = \tau_D$ it was shown that over a comparatively wide range of experimental conditions, the value of the ratio for 10 rows of nozzles varies between 2.8 and 3.0. When also taking into account the reduction of the size of the dead zone and the decrease of the τ_D values, the arrangement appears to be very advantageous (cf. Figs. 1—3). There remains the problem of perfect experimental verification of the assumed type of flow which should result in an efficient mixing of the glass melt at each of the nozzle rows. Even though the preliminary results of physical modelling seem to support the assumption [5], more extensive measurements are still required. A certain disadvantage is represented by the requirement for several transverse rows of nozzles one behind the other, which is quite demanding with respect to overall length and the total number of nozzles.

The present chapter will therefore be concerned with another arrangement which should eliminate the drawback. Its principle is based on creating an adequately extensive transverse flow in the melting zone by means of a central row of nozzles. In the melting zone, the forward and backward flow should combine with the transverse flow due to the nozzles. The transverse flow is assumed to be more extensive than the longitudinal one. Two longitudinally rotating cylindrical formations of glass melt will form in the melting zone, and the melt will move along spiral tracks inside the cylinders. The spiral or helical movement will result in an "averaging" of the original tracks in the furnace. In an ideal case the back flow could be completely eliminated and all of the glass melt would move towards the exit. In addition to this, the temperature in the melting zone would attain an average value, and the originally unfavourable $\bar{\tau}/\tau_{\text{pass}}$ ratio would be reduced. In order to assess at least approximately the advantage of such an arrangement, let us calculate the example of a rectrangular duct with a sectional area corresponding to that of a 'long tank' in the previous chapter. The following assumptions are made in the calculation:

a) The flow rate distribution in the longitudinal direction (component v_x) has the form of two paraboloids, the top one expressing the backward flow and the bottom one the forward flow.

b) The non-isothermal component is very small ($\tau_{\text{pass}} = \tau_{\text{tech. pass}} = \tau_D$); the temperature gradient is assumed in direction x only.

c) The bubbling nozzles in the central row are close enough one from the other, so that no backward flow towards the bottom will occur between them.

d) To simplify the calculation it is assumed that the transverse flow projections form concentric rectangles whose shape is identical with one half of the transverse duct sectional area, the centres of all the rectangles being situated at the intersections of the common diagonals.

e) The rate of transverse flow along a given path is independent of the place (however, the angular and circumferential rates of flow along the individual concentric tracks may differ).

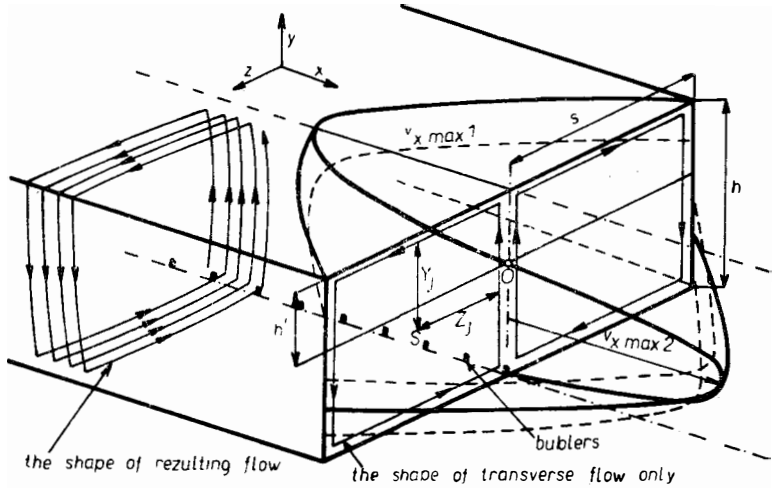

Fig. 4. Sectional view of the rectangular duct with indicated flow rate profiles in direction x, and with flow shapes.

The cross section of a rectangular duct with indicated flow rate profiles in direction x and the assumed shape of flow are shown in Fig. 4. Under the given conditions, an arbitrary point moving along an approximately spiral path (cf. the figure) will cover, during one revolution, a distance in direction x, given by the sum of ten partial distances s_i:

$$s_1 = -\frac{v_{x\max 1}}{12\,h'^2}\,\frac{\left(Y_j - \frac{h}{2} + h'\right)\tau_j}{(Y_j + Z_j)}\left[\frac{\left(\frac{s}{2} - Z_j\right)^2}{s^2} - 1\right]\cdot\left(Y_j - \frac{h}{2} + 2h'\right), \tag{3a}$$

$$s_2 = -\frac{v_{x\max 1}}{s^2}\,\frac{Z_j\,.\,\tau_j}{Y_j + Z_j}\left[\left(Y_j - \frac{h}{2}\right)^2\cdot\frac{1}{h'^2} - 1\right]\cdot\left(\frac{Z_j^2}{6} - \frac{3s^2}{8}\right), \tag{3b}$$

$$s_3 = -\frac{v_{x\max 1}}{12\,h'^2}\,\frac{\left(Y_j - \frac{h}{2} + h'\right)\tau_j}{(Y_j + Z_j)}\left[\frac{\left(\frac{s}{2} + Z_j\right)^2}{s^2} - 1\right]\cdot$$

$$\cdot\left(Y_j^2 + \frac{h^2}{4} - 2h'^2 - Y_j h' - Y_j h + \frac{hh'}{2}\right), \tag{3c}$$

$$s_4 = -\frac{v_{x\max 2}}{3(h' - h)^2}\,\frac{\left(Y_j + \frac{h}{2} + h'\right)^2\tau_j}{(Y_j + Z_j)}\left[\frac{\left(\frac{s}{2} + Z_j\right)^2}{s^2} - 1\right]\cdot\left(Y_j - h + \frac{h'}{2}\right), \tag{3d}$$

$$s_5 = -\frac{v_{x\max 2}}{s^2}\,\frac{Z_j\,.\,\tau_j}{(Y_j + Z_j)}\left[\left(\frac{h'}{2} - Y_j\right)^2\frac{4}{(h' - h)^2} - 1\right]\cdot\left(\frac{Z_j^2}{6} - \frac{3s^2}{8}\right), \tag{3e}$$

$$s_6 = \frac{v_{x\,\max\,x2}}{3(h'-h)^2} \frac{\left(Y_j + \frac{h}{2} - h'\right)\tau_j}{(Y_j + Z_j)} \left[\frac{\left(\frac{s}{2} - Z_j\right)^2}{s^2} - 1\right] \cdot$$
$$\cdot \left(Y_j^2 - \frac{h^2}{2} - \frac{h'^2}{2} - \frac{Y_j h}{2} - \frac{Y_j h'}{2} + \frac{h \,.\, h'}{2}\right). \tag{3f}$$

It will be shown that the ratio of paths in direction x in the individual concentric tracks is independent of the time of circulation (i. e. the rate of flow) a ong an arbitrary rectangular path. After an adequately long time τ the ratio of two paths s_k, s_j in direction x on two arbitrary rectangular paths, designated k and j, is given by the equation

$$\frac{s_k}{s_j} = \frac{n_k \tau_k \sum_{i=1}^{6} \text{const}_{ik}}{n_j \tau_j \sum_{i=1}^{6} \text{const}_{ij}}. \tag{4}$$

As it holds that

$$n_k = \frac{\tau}{\tau_k} \qquad \text{and} \qquad n_j = \frac{\tau}{\tau_j}, \tag{5}$$

one obtains after substitution

$$\frac{s_k}{s_j} = \frac{\sum_{i=1}^{6} \text{const}_{ik}}{\sum_{i=1}^{6} \text{const}_{ij}}. \tag{6}$$

$\sum \text{const}_{ik}$ and $\sum \text{const}_{ij}$ are independent of the time of circulation.

As follows from the last equation, the efficiency of this way of controlling the convection depends just on the ratio of the paths, that is the fastest path corresponding to the time of passage, and the path corresponding to the mean residence time:

$$\frac{s_{\text{pass}}}{\bar{s}} = \frac{v_{\text{pass}}}{\bar{v}} = \frac{\bar{\tau}}{\tau_{\text{pass}}}. \tag{7}$$

It is interesting to determine the values of these ratios for some flow rate profiles in direction x in the duct. For flow rate v_x increasing linearly with ordinate y (independently of z), the ratio $\bar{\tau}/\tau_{\text{pass}} = 2.25$; on introducing transverse flow it will hold that $\bar{\tau}/\tau_{\text{pass}} = 1$; for the parabolic flow rate profile including the forward flow only, it holds that the ratio $\bar{\tau}/\tau_{\text{pass}} = 2.25$; introduction of transverse rectangular flow will reduce the ratio to approximately 2.25; as is already known, if there is backward flow, the ratio $\bar{\tau}/\tau_{\text{pass}}$ is quite high (roughly between 8 and 10) as a result of recycling of considerable proportion of the glass melt. There is the question to what extent this ratio will change on introduction of transverse flow. The ratio will obviously be given by the shape of the flow rate profile in direction x. As for the case $m = 0$ the mean flow rate is simultaneously the rate corresponding to the so-called geometric residence time, i. e.

$$\bar{v} = v_{\text{geom}} = \frac{L}{\tau_{\text{geom}}} = \frac{L \,.\, V}{V}, \tag{8}$$

at a contant throughput the value of $\bar{v}$ is fixed and the ratio $\bar{\tau}/\tau_{pass}$ can only be reduced by raising the value of τ_{pass}, which decreasés significantly with the degree of back flow. For this reason, and in view of the averaging of paths after introduction of transverse flow, it would be advantageous to make the flow-rate profiles of both forward and backward flow as symmetrical as possible (the ideal case of $\bar{\tau}/\tau_{pass} = 1$ would be approached by a duct enclosed from above and having a small throughput). Generally, the seeking of the most favourable rate profiles is difficult, but the symmetry requirement helps us assess the profiles at least qualitatively.

In addition to the ratio of the two rates of flow, $v_{x\,max\,2}$ and $v_{x\,max\,1}$, a significant part will obviously be played by situating the level of zero rate in direction x for $y \neq 0$; $y \neq h$. It may be said that at small rates of flow (usual in tank furnaces), those with substantial differences between the values of $v_{x\,max\,1}$ and $v_{x\,max\,2}$ are not advantageous; the thicknesses of forward and backward flow can also be expected to show great differences. In that case, even when transverse flow has been introduced, one can expect the back flow to occur and reduce the value of τ_{pass}. An extremely unfavourable case will arise when the centre of the rotating transverse flow is located in the region of $v_{x\,max\,2}$ (cf. Fig. 4). Then the value of τ_{pass} will be roughly the same for the case with transverse flow and without it, and introduction of transverse flow will have no favourable effect.

To illustrate the problem, let us take the example of transverse flow on the assumption that the simplifying assumptions mentioned above hold. Let us compare two cases of melting with and without transverse flow, both 'little non-isothermal' in character. Similarly to the previous chapter, the melting takes place in a tank with a melting section 10 m in length, 4 m in width, a glass layer thickness of 1 m. At a distance of 2 m from the feed end, a row of bubbling nozzles is placed along the longitudinal axis. The model glass melt (cf. [1]) is refined with 0.7 % Na_2O in the form of Na_2SO_4, $r_{0\,max} = 0.2$ mm. The refining takes place in the extended section (cf. [9], p. 54). The mean temperature in the melting zone for both cases being compared amounts to 1300 °C; according to technological practice with

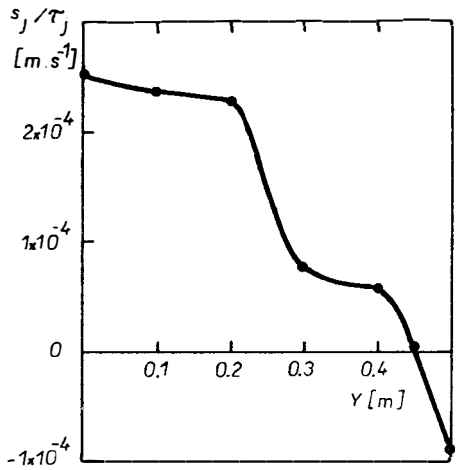

Fig. 5. Average rates of flow of glass melt in direction x along rectangular paths.

standard tanks, the dead zone assumed is $m = 0.2$ and the ratio $\tau_{pass} = 0.12\,\bar{\tau}$. The time of sand dissolution established in laboratory without bubbling was 274 min, and with bubbling 60 min. The time of dissolution in a tank will vary between these limit values, so that the calculation will be made for both cases. Melting without any reserve is assumed, so that the value of $v_{x\,max\,2}$ can be calculated. It is further assumed that the rate profile in direction x is not changed by the introduction of transverse bubbling. To be able to utilize the possible reserve due to an increase in τ_{pass} (the throughput will remain unchanged), the tank can be shortened, in a favourable case, so as to perform without any reserve even with transverse flow. Using simplified calculations, it is possible to estimate the value of h' in equations (3a—f) at 0.4. The calculated profiles of the mean flow rate of the individual points along rectangular paths in direction x are plotted in Fig. 5. The diagram reveals the existence of a minute backward flow close to $Y \to 0.5$, $Z \to 1$; the maximum speed in direction x is attained by the center of the rectangular flow whose path becomes critical. The value of the $\bar{\tau}/\tau_{pass}$ ratio for this critical path decreases from the original 10 to 4.23. In this instance, the tank can be shortened from 10 m down to 6.2 m to make it again operate without any reserve. The specific energy consumption will decrease, and the specific output increase correspondingly. For the case of sand dissolution time reduced to 60 minutes, the tank length would be cut to approximately 3 m, and the ratio $\bar{\tau}/\tau_{pass}$ would not change.

It is of course possible to consider another case when instead of shortening the tank one would, while introducing transverse flow, increase the tank throughput so that the tank would again operate without any reserve. In that case it is assumed that the shape of the flow rate profile in the direction of x would be maintained (but not the flow values) on introduction of bubbling. Two opposite effects would in fact occur: that of increased throughput will promote forward flow, but that of increased temperature gradient (cooling the melt at the charge feeder) will act towards maintaining the shape of flow. Even in this case will the $\bar{\tau}/\tau_{pass}$ ratio remain of course the same, being dependent solely on the shape of the flow rate profile in direction x. The results of all of the calculations are listed in Table VI.

Table VI

Tank	Length of melting zone [m]	Q [kJ/kg]	P [t/(24 h m³)]	Bubbling
Original	10	8 955	1.20	no
Shortened, with higher τ_0 value	6.2 (5.45)	6 495 (6 030)	1.96 (2.20)	yes
Shortened, with lower τ_0 values	3.0 (2.75)	4 078 (3 909)	4.0 (4.36)	yes
Original, with higher τ_0 value, higher throughput	10.0	5 608 (5 040)	2.31 (2.75)	yes
Original, with lower τ_0 value, higher throughput	10.0	3 125 (2 977)	10.50 (12.60)	yes

The table indicates that the effect is always discernible, even though mostly not so obvious as in the case of bubbling from transverse rows of nozzles. This is particularly due to the fact that in this case one has to expect a smaller effect of bubbling on the value of τ_D. However, the arrangement has the advantage of a substantially smaller number of bubbling nozzles.

When then the symmetry of flow-rate distribution in direction x is improved by setting the level of zero flow rates in direction x to one half the glass melt layer thickness ($h' = h/2$), the resulting ratio $\bar{\tau}/\tau_{\text{pass}}$ will decrease to 3.5. The decrease of specific energy consumption and the increase in throughput is indicated by the values in brackets.

The main problem is obviously to achieve as flat 'mean flow rate' profiles as possible in direction x while not knowing the exact shape of the rate profile components in direction x (one can call this the attainment of a quasipiston flow). It would obviously be advantageous to introduce suitable agitation in the vertical direction (e. g. with the use of several low-output nozzles) at the line $y = 0$, $z = 1/4\,s$ and $3/4\,s$, thus re-averaging the already averaged spiral paths. The advantage would be based on further reduction of the $\bar{\tau}/\tau_{\text{pass}}$ ratio towards unity, and on greater efficiency of bubbling with respect to sand dissolution.

In practice, when the conditions are considerably non-isothermal in character (there is a temperature gradient in vertical direction) it is also necessary to consider the significant favourable effect of temperature averaging of the individual tracks due to introduction of transverse flow.

CONCLUSION

As indicated by the results of the present study, there are realistic possibilities of substantially intensifying the melting process in the melting zone. The two cases using agitation of the glass melt by transverse rows of nozzles or a longitudinal one were dealt with only semiquantitatively. The prospects of such arrangements are obvious, as are the problems involved. It is first of all necessary to create a mathematical model of the melting zone, which would be capable of providing a precise picture of the flow and could be used as evidence for practical applicability of such and other similar arrangements. The two cases are thus just a couple of the many possibilities that can be resolved by means of models.

References

[1] Němec L.: Silikáty *32*, 193 (1988).
[2] Němec L., Laurentová S.: Silikáty *32*, 313 (1988).
[3] Němec L., Laurentová S.: Silikáty *33*, 106 (1989).
[4] Němec L., Laurentová S.: Silikáty (in press).
[5] Auerbeck J.: Personal communication, State Glass Research Institute, Hradec Králové.
[6] Němec L.: Sklář a keram. *29*, 103 (1979).
[7] Němec L.: Sklář a keram., *29*, 144 (1979).
[8] Sawai I., Takahashi K., Kunugi M., Taumagari A.: Comptes Rendus IIa, VII. Congr. Internat. du Verre, paper 58, Bruxelles (1965).
[9] Laurentová S.: Diploma Thesis, Department of the Technology of Silicates, Institute of Chemical Technology Prague, (1988).

List of Symbols

h — total height of glass melt flow [m]

h' — height of back flow [m]

— number of recycles above the l-th row of nozzles

m_0 — τ_D/τ (integer obtained by rounding the ratio upwards)

m, m_1, m_2 — dead zone in the melting and refining sections

n_k, n_j — number of recycles along the k-th and j-th path during time τ, $\sum$ const ik, $\sum$ const ij — sum of constants including the right-hand sides of equations (3a—f) except the values of τ_k, τ_j — the times of recycles along the k-th and the j-th path

$r_{0\,max}$ — the initial radius of the largest sand grain [mm]

s — half the duct width [m]

$\bar{s}$ — track per time τ corresponding to the mean residence time [m]

s_1 — path travelled by an element of glass melt along a part of spiral track during one cycle [m]

s_{pass} — path travelled during time τ corresponding to the time of passage [m]

v_{geom} — the so-called geometrical speed of movement of the glass melt through the melting zone [ms^{-1}]

$v_{x\,max1}, v_{x\,max2}$ — maximum components of rate of flow in direction x

$v_{pass}, \bar{v}$ — flow rate in direction x corresponding to the time of passage and the mean residence time (ms^{-1}]

A_{il} — integer coefficients used in the resolving of equation (1) according to instruction

L — length of the melting zone or duct [m]

N_1' — concentration of sand grains in the melt after the melting time $(i - 1)\,\tau_i + \tau_i/2$ established in laboratory [number per kg]

P — throughput of the melting zone [t/(24 hm^3)]

P' — the probability with which the glass melt will pass to the next row of nozzles after the first recycle above the row

Q — specific energy consumption of melting [kJ kg^{-1}]

ΔQ_M — the amount of energy required for heating 1 kg of glass melt from melting temperature in the first melting zone to the refining temperature in the second melting zone [kJ kg^{-1}]

$X_{m,\,l+1}$ — concentration of undissolved sand grains [number per kg]

X_N — admissible standard concentration of undissolved sand grains behind the last row of nozzles [number per kg]

V — volume of the melting zone [m^3]

$\dot{V}$ — throughput by volume through the melting tank [m^{3}s^{-1}]

Y_j, Z_j — half width and height of the respective j-th rectangular tracks in cross section [m]

τ_D — time of sand dissolution [s]

τ_i — the mean time of recycling of the melt above one row of nozzles [s]

τ_{geom} — the so-called geometrical time of residence [s]

τ_j — time of one recycle along j-th rectangular track [s]

$\bar{\tau}$ — mean residence time of glass melt in a continuous melting tank [s]

τ_{pass} — the shortest time of passage of a melt element through the tank [s]

τ_R — the time required for refining/elimination of bubbles (seed), [s]

$\tau_{tech\ pass}$ — technological time of melting along the fastest path [s]

HLAVNÍ TECHNOLOGICKÉ CHARAKTERISTIKY SKLÁŘSKÝCH TAVICÍCH PROSTORŮ Z HLEDISKA PRŮBĚHU TAVICÍHO PROCESU

ČÁST V. VLIV USPOŘÁDÁNÍ PROUDĚNÍ POMOCÍ PROBUBLÁVÁNÍ

Lubomír Němec

Ústav chemie skelných a keramických materiálů ČSAV, 120 00 Praha

Výsledky předcházejících prací [1—4] ukazují velké ovlivnění měrné energetické spotřeby a výkonu tavicího prostoru uspořádáním proudění. V práci byly pomocí odhadnutých tvarů proudění řešeny dva případy: Tavicí prostor s několika příčnými řadami probublávacích trysek a tavicí prostor s jednou řadou probublávacích trysek v podélné ose. Pro první případ vypočtené hodnoty ukazují ve srovnání s případem bez probublávání značné snížení měrné energetické spotřeby a zvýšení výkonu (Obr. 1—3. a Tab. II, IV, V). Pro případ podélné řady probublávacích trysek (Obr. 4.) jsou výsledky rovněž příznivé (Tab. VI). Obojí uspořádání by mělo význam především pro tavení za nepříliš vysokých teplot výhodných z ekologického hlediska. Podrobněji je nutno taková uspořádání řešit pomocí matematických modelů tavicích prostorů.

Obr. 1. Měrná energetická spotřeba a výkon v závislosti na teplotě pro „dlouhou vanu", modelová sklovina (74 % SiO_2, 16 % Na_2O, 10 % CaO), 0,7 % Na_2O j. Na_2SO_4, r_{0max} = 0,20 mm.
○ — *bez probublávání, $m_1 = 0{,}9$; $m_2 = 0$*
× — *s probublávánim, $m_1 = 0$; $m_2 = 0{,}9$*
\+ — *s probublávánim, $m_1 = 0$: $m_2 = 0$*

Obr. 2. Měrná energetická spotřeba a výkon v závislosti na teplotě pro „dlouhou vanu", modelová sklovina, 2 % Na_2O j. NaCl, r_{0max} = 0,20 mm.
○ — *bez probublávání, $m_1 = 0{,}9$; $m_2 = 0$*
\+ — *s probublávánim, $m_1 = 0$: $m_2 = 0$*

Obr. 3. Měrná energetická spotřeba a výkon v závislosti na konc. NaCl *pro „dlouhou vanu", modelová sklovina, 1300 °C, r_{0max} = 0,20* mm.
○ — *bez probublávání, $m_1 = 0{,}9$; $m_2 = 0$*
× — *s probublávánim, $m_1 = 0$; $m_2 = 0$*

Obr. 4. Příčný řez pravoúhlým kanálem s vyznačením profilů rychlostí ve směru x a tvary proudění.

Obr. 5. Průměrné rychlosti posunu skloviny ve směru x na obdélníkových drahách.

Němec:

ОСНОВНЫЕ ТЕХНОЛОГИЧЕСКИЕ ХАРАКТЕРИСТИКИ ВАРОЧНЫХ ЗОН С ТОЧКИ ЗРЕНИЯ ХОДА ВАРОЧНОГО ПРОЦЕССА

V. ВЛИЯНИЕ УПОРЯДОЧЕНИЯ КОНВЕКЦИИ С ПОМОЩЬЮ БАРБОТАЖА

Лубомир Немец

Институт химии стеклянных и керамических материалов ЧСАН, Липова 5, 120 00 Прага 2

Результаты предшествующих работ [3—4] показывают, что на удельный расход энергии и мощность варочной зоны огромное влияние оказывает упорядочение конвекции. В предлагаемой работе решаются на основе оценки форм конвекции два случая: варочная зона с несколькими поперечными рядами барботажных форсунок и варочная зона с одним рядом барботажных форсунок в продольной оси. В первом случае расчитанные величины показывают в сравнении со случаем без барботирования значительное понижение удельного расхода энергии и повышение мощности (см. рис. 1.—3. и табл. II, IV, V). В случае продольного ряда барботажных форсунок (см. рис. 4.) результаты также положительны (см. табл. VI). Как первое, так и второе упорядочение имело бы свое значение прежде всего в случае варки при не очень высоких температурах, оказывающихся пригодными с экологической точки зрения. Такое упорядочение требует более подробного решения с помощью математических моделей варочных зон.

Рис. 1. Удельный расход энергии и мощность в зависимости от температуры для „длинной ванны“; модельная стекломасса (74 % SiO_2, 16 % Na_2O, 10 % CaO, 0,7 % Na_2O. Na_2SO_4, r_0 макс. = 0,20 мм; о — без барботажа, $m_1 = 0{,}9$, $m_2 = 0$, × — с баботажем, $m_1 = 0$, $m_2 = 0{,}9$ + — с барботажем, $m_1 = 0$, $m_2 = 0$.

Рис. 2. Удельный расход энергии и мощность в зависимости от температуры для „длинной ванны“, модельная стекломасса, 2 % Na_2O . NaCl, r_0 макс. = 0,20 мм, о — без барботажа, $m_1 = 0{,}9$, $m_2 = 0$, + — с барботажем, $m_1 = 0$, $m_2 = 0$.

Рис. 3. Удельный расход энергии и мощность в зависимости от концентрации NaCl для „длинной ванны“, модельная стекломасса, 1 300 °C, r_0 макс. = 0,20 мм, о — без барботажа, $m_1 = 0{,}9$, $m_2 = 0$, × — с барботажем, $m_1 = 0$, $m_2 = 0$.

Рис. 4. Поперечное сечение прямоугольным каналом с обозначением профилей скоростей в направлении x и формы конвекции.

Рис. 5. Средние скорости перемещения стекломассы в направлении x на прямоугольных трассах.